compounds

MDPI

Article

Preparation and Characterizations of Curcumin Protection and Delivery System Using Linear Dextrin

Huifang Xie [1,*], Litao Ma [1], Yanan Li [1], Jun Fu [1], Zhongxian Li [1], Xuejun Yu [1] and Qunyu Gao [2,*]

[1] Institute of Chemistry, Henan Academy of Sciences, Zhengzhou 450002, China
[2] Carbohydrate Laboratory, School of Food Science and Engineering, South China University of Technology, Guangzhou 510640, China
* Correspondence: xiehf0213@gmail.com (H.X.); qygao@scut.edu.cn (Q.G.); Tel.: +86-15736782739 (H.X.); +86-13660261703 (Q.G.); Fax: +86-020-87113848 (Q.G.)

Abstract: In this work, linear dextrins (LDs) with the fragment F-40 (DP = 31.44) were fabricated from waxy potato starch through pasteurization and enzymatic debranching by pullulanase and then separated and extracted by ethanol solutions with different concentrations. The LDs were used to encapsulate hydrophobic ligand curcumin to develop a controlled release system that would increase its flavor in food and functions in medicines. The physicochemical properties and the encapsulation mechanism of the inclusion complexes were investigated. It was found that the loading capability for curcumin, the encapsulation rate, and the yield of the complexes depended on the molecular weight of LD. The yield of the LD-Cur complex, its encapsulation rate, and loading of curcumin were 19.86%, 25.81%, and 29.52 μg/mg, respectively, while the yield of the F-40-Cur complex, its inclusion rate, and loading curcumin reached up to 75.98%, 29.97%, and 37.52 μg/mg, respectively. There were both hydrogen bonding and hydrophobic interactions between LD and curcumin, while hydrogen bonding interactions were predominant between F-40 and curcumin. Curcumin was presented in the complex in an amorphous form. The photothermal stability of curcumin increased after being complexed with LD and further enhanced significantly with F-40. The release of curcumin in the intestine was achieved much more effectively.

Keywords: curcumin; encapsulation; LD; inclusion complexes; potential curcumin delivery system

Citation: Xie, H.; Ma, L.; Li, Y.; Fu, J.; Li, Z.; Yu, X.; Gao, Q. Preparation and Characterizations of Curcumin Protection and Delivery System Using Linear Dextrin. *Compounds* **2022**, 2, 353–366. https://doi.org/10.3390/compounds2040029

Academic Editor: Juan C. Mejuto

Received: 9 October 2022
Accepted: 15 November 2022
Published: 16 November 2022

1. Introduction

Turmeric is a spice that has attracted a lot of interest from the medical, scientific, and culinary communities. Turmeric is traditionally used as a medicinal herb in Asian cultures due to its antioxidant, anti-inflammatory [1,2], antimutagenic, antibacterial [3,4], and anticancer properties [5,6]. Curcumin, the principal constituent of turmeric, is a polyphenol that can target a variety of signaling molecules while exhibiting activity at the cellular level, which explains its multiple health benefits [7]. However, the challenge with ingestion of curcumin is its poor bioavailability [8], which results in its malabsorption and rapid metabolism and clearance [7,9].

To overcome these limitations, the application of appropriate release systems, such as hydrogels, dendrimers, liposomes, and micro- and nanoparticles, have been used for the delivery of curcumin [10,11]. In recent years, targeted and triggered drug delivery systems accompanied by nanoparticle technologies have become prominent solutions for improving therapeutic drug bioavailability [12]. Nanoparticle-based drug delivery systems will likely be suitable for highly hydrophobic drugs, such as curcumin, thus avoiding the drawback of poor water solubility. Nanoparticle-based curcumin delivery systems are still in their infancy, and there is still much progress to be made in this field [13,14]. Bisht et al. reported the synthesis, structural characterization, and applications of curcumin nanoparticles with a particle size under 100 nm [15]. Tiyaboonchai et al. [16] developed and characterized

solid lipid nanoparticles (SLNs) loaded with curcumin for topical application. The results showed that curcumin-loaded SLNs with a particle size of 450 nm were stable at room temperature for 6 months and prolonged the in vitro release of curcumin up to 12 h. In addition, by adding curcumin to this unique dosage form, the light and oxygen sensitivity of curcumin was greatly reduced. Sun et al. [17] from Jiangnan University performed an ethanol-hydrochloric acid pretreatment of common corn starch followed by pullulanase debranching and phase separation in a DMSO-ethanol binary system after which selected fragments were used to embed curcumin. Linear dextrin (LD)/curcumin complexes were prepared by the coprecipitation method. The effects of reaction time were investigated, including weight ratio, degree of polymerization (DP), encapsulation rate, and complex yield. For LD with longer DP, the yield, curcumin payload, and inclusion rate reached 73.98%, 28.76 μg/mg, and 23.81%, respectively. Overall, longer LDs produced higher yields and better retained the activity of curcumin compared to shorter LDs. However, lower complex yields were produced. Linear dextrin (LD) was prepared using waxy potato starch debranched with pullulanase. Various LDs were separated on the basis of their differential solubility in aqueous/ethanol solutions of different volumetric ratios. Three LD products—LD fabrications with 40% ethanol (F-40); LD fabrications with 50% ethanol (F-50); and LD fabrications with 60%, 70%, and 80% ethanol (F-M)—were obtained with an average degree of polymerization (DP) values of 31.44, 21.84, and 16.10, respectively. This was the origin of F-40 according to our previous work [18].

In this study, F-40 with a narrower molecular weight and an average polymerization degree of 31.44 was used to encapsulate curcumin to prepare F-40-curcumin nanocomplexes. Moreover, the light stability and in vitro release properties of the nanocomplexes were investigated in order to characterize potential improvement in the bioavailability of curcumin. The method we used includes pullulanase and ethanol, and it is a green method. The results of this study may provide valuable data for research on encapsulation mechanism for curcumin and linear dextrin with different, narrower molecular weights. Moreover, the results may help to expand the commercial potential and application of starch-based nanocarriers in the pharmaceutical and food industries.

2. Materials and Methods

2.1. Materials

Curcumin (purity > 98%) was obtained from Guangzhou LES Biological Technology Co., Ltd. (Guangzhou, China). Trypsin (pancreatin, P7545) was supplied by Sigma-Aldrich Corporation (Shanghai, China). Pepsin (pepsin, P7000) was supplied by Sigma-Aldrich Corporation (Shanghai, China). Other chemical reagents of analytical grade purity were purchased from Tianjin Damao Chemical Reagent Factory (Tianjin, China). Sample F-40 was prepared according to Xie et al. [18] with minor modification.

2.2. Preparation of Linear Dextrin-Curcumin Nanocomplexes

LD-curcumin complexes were prepared using the coprecipitation method described by Marcolino et al. [19] with slight modifications. Curcumin (4 mg/mL) was dissolved in pure anhydrous ethanol to prepare a stock solution. LD (10 mg/mL) powder was dissolved in distilled water to achieve a concentration of 10 mg/mL. The resulting suspension was heated to 100 °C for 30 min and then cooled to 80 °C. Then, different volumes of the curcumin-ethanol solution (at a ratio of 1:10) were added to the LD solution with gentle mixing at 80 °C for 2 h. The mixture was then allowed to stand for 12 h at 4 °C. The resulting precipitate was centrifuged (12,000× *g*, 10 min, 4 °C), washed 3 times with 50% (*v*/*v*) ethanol, and then dried in an oven at 40 °C. As a control sample, LD solutions without curcumin were also prepared and used for further analysis. All samples were prepared in triplicate, and the resulting complexes were stored in brown glass vials. The yield of the

complex was calculated by dividing the weight of the complex from the total weight of curcumin and LD using Equation (1):

$$\text{Yield} = \frac{\text{W}}{\text{W}_1 + \text{W}_2} \times 100\% \quad (1)$$

where W_1, W_2, and W are the masses (g) of LD, curcumin, and LD-curcumin complexes, respectively. The blank sample was the pure LD solution, and the control sample was the LD-curcumin physical mixture.

2.3. Determination of Curcumin Loading and Encapsulation Rate

To determine the curcumin content of the LD-curcumin complex, a fixed amount of each powder was diluted in anhydrous ethanol and then mixed for 5 min. The mixture was then treated in an ultrasonicator for 10 min to extract the curcumin and centrifuged at 5000× *g* for 10 min. The extraction process was repeated three times, and the curcumin-containing supernatant was combined. Then, the concentration of curcumin in the supernatant was measured by a TU-1900 UV-visible spectrophotometer at 419 nm. The effective loading (X, μg/mg) and the encapsulation rate of curcumin (Y, %) were calculated by Equations (2) and (3), respectively:

$$\text{X} = \frac{\text{C} \times \text{N} \times \text{V}}{\text{m0}} \times 100\% \quad (2)$$

$$\text{Y} = \frac{0.01 \times \text{m1} \times \text{X}}{\text{m2}} \times 100\% \quad (3)$$

where C (μg/mL) is the curcumin content of the dilute composite solution determined from the curcumin standard curve (y = 0.1490, x-0.0001, R^2 = 0.9998; x and y correspond to the curcumin concentration and absorbance in μg/mg, respectively), N is the dilution factor of the supernatant, V (mL) is the total volume of anhydrous ethanol, m0 (mg) is the mass of the weighed complex sample, m1 (mg) is the mass of the LD-curcumin complex, and m2 (mg) is the mass of added curcumin.

2.4. XRD Analysis

X-ray diffractograms (XRD) of powdered curcumin, LD, LD-curcumin physical mixture, and LD-curcumin complex as well as F-40, F-40-Cur mixture, and F-40-Cur complex were collected using an X-ray diffractometer (D8 Advance, Bruker Co., Germany) operating at 30 kV and 10 mA and using Cu-Kα radiation (1.5406 Å). The samples were scanned from 3 to 60° (2θ) at a scan rate of 4°/min, and the resulting data were analyzed using MDI Jade 5.0 software (Materials Data Inc., Livermore, CA, USA).

2.5. FT-IR Analysis

The intermolecular interactions of the sample curcumin, LD, LD-curcumin physical mixture, and LD-curcumin complex as well as F-40, F-40-Cur mixture, and F-40-Cur complex were analyzed by FT-IR (Vector 33, Bruker Co., Germany). Specifically, the samples were mixed with KBr at a ratio of 1:100 to 1:50, and the dried samples were pressed into pellets for spectral acquisition. Next, scanning was performed, and the test was performed with a KBr slice as a blank background. The scan range was generally chosen from 400 to 4000 cm^{-1}, the number of scans was set to 64, and the resolution of the test was set to 4 cm^{-1}.

2.6. TEM Analysis

The morphology of the complexes was observed using transmission electron microscopy (TEM; JEM1400 Plus, JEOL, Tokyo, Japan) at an accelerating voltage of 80 kV. The 0.01% (*w*/*v*) sample suspension was sonicated at room temperature for 5 min and then drop-cast onto a copper mesh coated with carbon film for observation.

2.7. Thermal Stability Analysis

The thermal properties of pure curcumin, LD, LD-curcumin physical mixture, and LD-curcumin complex as well as F-40, F-40-Cur mixture, and F-40-Cur complex were characterized using a thermogravimetric analyzer (TG-DSC, STA449F3, Selb, Germany). The instrument was operated in a nitrogen atmosphere with a nitrogen flow rate of 20 mL/min and a heating rate of 10 °C/min in the range of 50 to 500 °C.

2.8. Photochemical Stability Analysis

The photochemical stability of the pure curcumin sample, LD, LD-curcumin mixture, and LD-curcumin complex as well as F-40, F-40-Cur mixture, and F-40-Cur complex powder was evaluated according to the procedure described by Patel, Hu, Tiwari, and Velikov [20] with some modifications. Powdered samples of curcumin and LD-curcumin complexes were subjected to UV light (368 nm) for 2, 5, 10, 24, 48, and 60 h in a dark box. The distance between the sample and the UV block was set to 8 cm. The curcumin content in the samples was measured by UV-visible spectroscopy at 419 nm.

2.9. In Vitro Simulation of Gastrointestinal Digestion Characterization

The preparation of gastric and small intestinal fluids was carried out as previously described [21], maintaining the entire simulated gastrointestinal environment isolated from oxygen and at a constant temperature of 37 °C. The release of curcumin from the complex under gastrointestinal stimulation conditions was assessed according to the method described by Pereira et al. [21] with some modifications. Briefly, 100 mg of sample LD-curcumin complex and 20 mg of F-40-Cur complex were incubated separately in 25 mL of simulated gastric fluid (SGF, containing 0.05% Tween 80, and 9 mg/mL pepsin) while stirring at 37 °C (95 rpm). After 60 min of incubation, the digestion solution was adjusted to pH 6.8 using 0.5M NaOH, and simulated intestinal digestion (60–180 min) was initiated by the addition of simulated intestinal fluid (SIF, containing 0.05% Tween 80 and 7.2 mg/mL trypsin). Throughout the digestion, reaction mixtures were collected at the following time intervals: 5, 15, 30, 45, 60, 90, 120, 150, and 180 min. Curcumin was extracted from these mixtures, and the in vitro simulated release profiles of the samples were determined as described above.

2.10. Statistical Analysis

Differences between multiple group means were analyzed by one-way analysis of variance (ANOVA) using SPSS 17.0 and Origin 9.0, and Duncan's multiple range tests were performed. $p < 0.05$ for ANOVA data was considered statistically significant. The means were from three experiments.

3. Results and Discussion

3.1. XRD Results

In the presence of suitable complexing agents, straight-chain starches can form a single-helix conformation with 6, 7, and 8 glucose units per turn, similar to the stacking of α-, β-, and γ-cyclodextrins, respectively. For β-cyclodextrin (β-CD), complexes are formed between curcumin and β-cyclodextrin or poly(β-CD), where the aromatic ring of curcumin is contained in the cavity of β-CD [22]. Considering the similarity of the helical structure of β-CD and straight-chain starch, curcumin can enter the helical cavity of straight-chain starch and form a complex with straight-chain starch. Therefore, in order to fully understand the interaction of LD and curcumin, the crystalline properties of curcumin in the LD matrix were detected by X-ray diffraction.

Figure 1A shows the XRD patterns of LD, curcumin, LD-curcumin mixture, and LD-curcumin complex, while the XRD patterns of F-40, F-40-Cur mixture, and F-40-Cur complex are shown in Figure 1B. As shown in Figure 1A,B, both LD and F-40 showed characteristic diffraction peaks at 5.6, 17.0, 22.0, and 24.2°, indicating the presence of B-type crystal structures. This result is in agreement with the findings of previous studies

that a B-type crystalline structure is typical for retrograded straight-chain starch [23]. In addition, the XRD pattern of the pure curcumin sample showed many spikes (8.9, 12.2, 14.6, 17.3, and 24.5°), which reflected its crystallinity. The characteristic diffraction peaks of the LD-curcumin complex appeared at 7.2, 8.3, 10.1, 14.2, 19.8, and 22.1°, which indicated that curcumin was still present in the LD-curcumin complex in crystalline form. The main crystalline form of the LD-curcumin complex resembled the crystalline structure of curcumin, even though the diffraction pattern of the LD-curcumin complex contained faint diffraction peaks characteristic of the V crystalline structure (2θ = 7.5, 13.3, and 14.4°), presumably due to the low loading of LD on curcumin. However, the F-40-Cur complex did not show a distinct curcumin crystalline peak, indicating that curcumin had been converted to the amorphous form. A similar phenomenon was observed by Cohen et al. [24]. For the LD-curcumin complex, the B-peaks dominated, although characteristic V-shaped peaks (2θ = 7.5, 13.3, and 14.4°) were also present. By comparison, the characteristic V-type crystalline structure in the F-40-Cur complex was found to be significantly stronger than that of the LD-curcumin complex, which was consistent with the results for curcumin loading capacity and directly indicated that the molecular chain length of F-40 was more favorable for the formation of its complexes. This difference can be mainly attributed to the different molecular weights of LD.

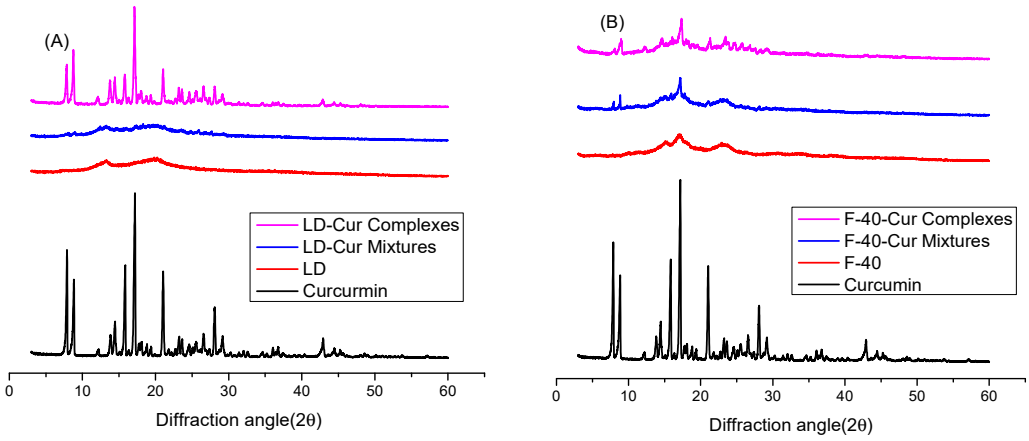

Figure 1. The XRD patterns of (**A**) curcumin, LD, LD-Cur mixtures, and LD-Cur complexes and (**B**) F-40, F-40-Cur mixtures, and F-40-Cur complexes.

3.2. FT-IR Results

The FTIR spectra of the pure curcumin sample, LD, LD-curcumin mixture, and LD-curcumin complex as well as F-40, F-40-Cur mixture, and F-40-Cur complex are shown in Figure 2. F-40 and LD exhibited the same FT-IR pattern due to similarities in their molecular structure. The broad peaks at 3385 and 2929 cm^{-1} were attributed to the -OH stretching vibration and the asymmetric stretching of CH originating from CH_2, respectively. Moreover, the strong peak at 1652 cm^{-1} corresponded to the bending vibration of -OH. In the curcumin spectrum, the most obvious carbonyl region (1800 to 1650 cm^{-1}) had no band, indicating that curcumin existed in the keto-enol interconversion isomeric form. The curcumin spectrum showed a sharp peak at 3509 cm^{-1} due to the phenol-OH stretching vibration. In addition, stretching vibrations at 1628 (vibrational C=O and C=C), 1604 (stretching vibration of the curcumin benzene ring), 1508 (CO and CC vibrations), 1429 (bending vibration of olefin CH), 1282 (stretching vibration of aromatic CO), and 1026 (stretching vibration of COC) cm^{-1} were noted.

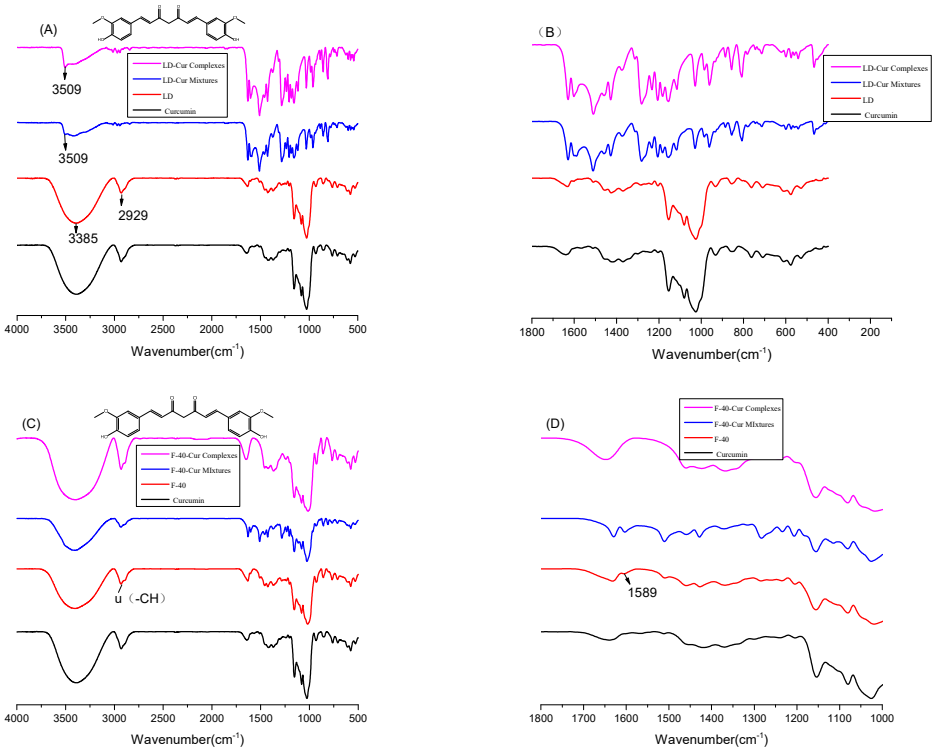

Figure 2. (**A**) The FT-IR patterns of curcumin, LD, LD-Cur mixtures, and LD-Cur complexes. (**B**) An enlargement of (**A**) at a wavelength range of 1800–200 cm^{-1}. (**C**) The FT-IR patterns of F-40, F-40-Cur mixtures, and F-40-Cur complexes. (**D**) An enlargement of (**C**) at a wavelength range of 1800–1000 cm^{-1}.

The FT-IR spectra of the physical mixture of LD-curcumin complex exhibited characteristic peaks corresponding to LD and curcumin. In contrast, the spectrum of the F-40-Cur complex showed some significant changes compared to the spectrum of the F-40-Cur mixture, which usually corresponds to the interaction of curcumin with the wall material [25]. Although peaks were observed at 1628 and 1508 cm^{-1}, the 3509 cm^{-1} spike belonging to the curcumin phenol -OH disappeared in the spectrum of the LD-curcumin complex.

Previous studies have suggested that hydrogen bonding is the main intermolecular interaction force between phenolic compounds and starch [26]. In our study, the phenol-OH group of curcumin and the OH group of the glucose unit may be involved in the formation of hydrogen bonds, as shown in the FT-IR spectral results. However, the phenol-OH of curcumin disappeared from the spectra of the F-40-Cur mixture and complexes. One possible reason for this may be due to the low weight ratio of curcumin to F-40, resulting in the characteristic peak of curcumin being covered by F-40. Notably, the peak at 1604 cm^{-1} corresponded to stretching of C=C of the aromatic ring of curcumin, which showed a shoulder peak at 1589 cm^{-1} in the spectrum of the F-40-Cur complex. This result suggests that the interaction seems to have occurred due to the entry of one or both benzene rings of curcumin into the helical cavity of F-40 (Figure 3).

Similar phenomena in curcumin-β-cyclodextrin complexes were reported by Tang et al. [27] and Mangolim et al. [2]. As for the differences in the FT-IR spectra of LD-curcumin complexes, they can be attributed to the degree of polymerization of LD. In summary, the intermolecular interactions between LDs and curcumin were mainly related to the benzene ring of curcumin, and it was speculated that hydrophobic interactions and hydrogen bonding were mainly between LD and curcumin, while the hydrogen bonding interactions were mainly between F-40 and curcumin.

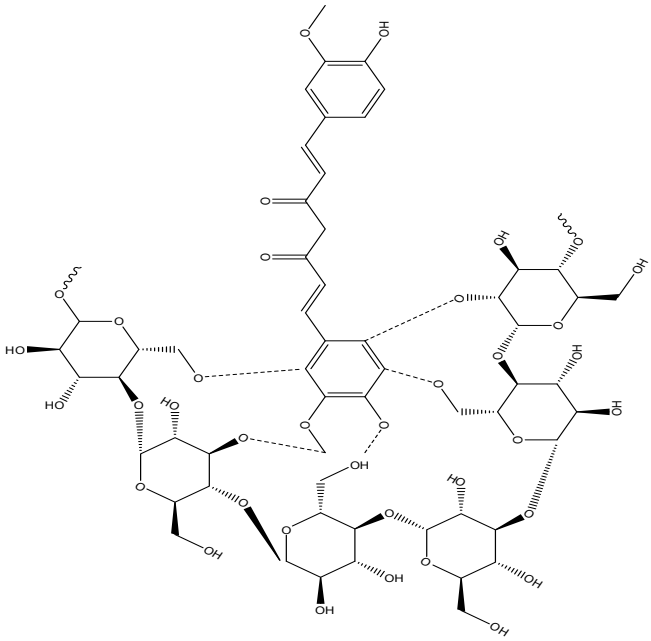

Figure 3. Molecular structure diagram of the F-40-Cur inclusion compound. The front view of the F-40-Cur inclusion compound, with dashed lines (- - - - - -) representing hydrogen bonding.

3.3. TEM Results

Figure 4 shows the transmission electron microscopy patterns of the LD-curcumin complex (left) and the F-40-Cur complex (right). Figure 4 (left) shows that the complexes of ungraded LD with curcumin were in the nanoparticle state, and the LD-curcumin complexes (left) were similarly close to containing nanoparticles with a roughly spherical shape and a diameter of about 50–80 nm. A small portion of nanoparticles aggregated and formed a grape-like structure, which is consistent with previous findings [28]. For F-40, its complex with curcumin was pale yellow in color and did not exhibit a distinct granular structure. In addition, Figure 4 (right) shows that the particle shape of the complex formed by long-chain F-40 and curcumin was larger, and the surface adhesion was more serious (about 70–80 nm). This difference was mainly related to the water solubility of LD. Klaochanpong et al. reported that debranched starch samples containing shorter linear chains showed higher solubility [29]. Therefore, the nongranular structure of F-40 complexes may be related to the molecular weight of LD. The LD sample had a higher percentage of shorter chains compared to the F-40 sample. Thus, LD exhibited excellent dispersion in water but a low ability to wrap curcumin molecules to form particle complexes.

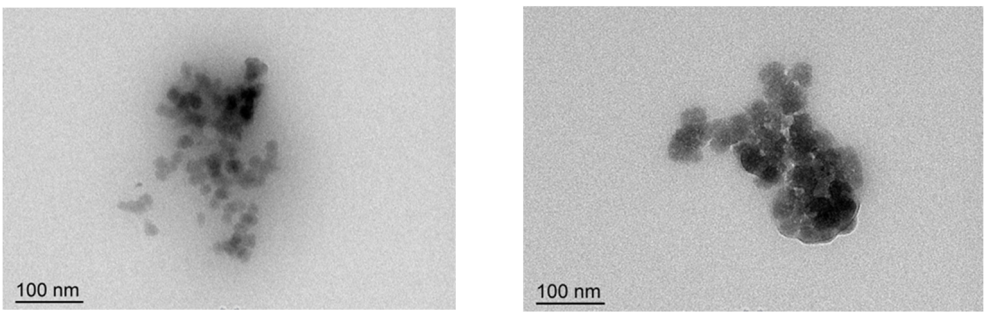

Figure 4. The TEM of LD-Cur complexes (**left**) and F-40-Cur complexes (**right**).

3.4. DSC-TG Results

The thermodynamic properties of the sample curcumin, LD, LD-curcumin mixture, and LD-curcumin complex as well as F-40, F-40-Cur mixture, and F-40-Cur complex are

shown in Figure 5. The LD and F-40 samples showed heat absorption peaks at 208.9 and 275.6 °C, respectively, corresponding to their melting points. This difference was related to differences in molecular size and arrangement, further confirming the effect of DP. The DSC spectrum of curcumin showed a heat absorption peak at 185 °C, which is the melting point of curcumin crystals [19]. While the heat absorption peak of curcumin was still present in the temperature spectrum of the LD-curcumin complex, the peak corresponded to the melting process of the amorphous LD in which LD is hardly complexed with curcumin during the coprecipitation process. This result was consistent with the graphical analysis of the previous XRD tests.

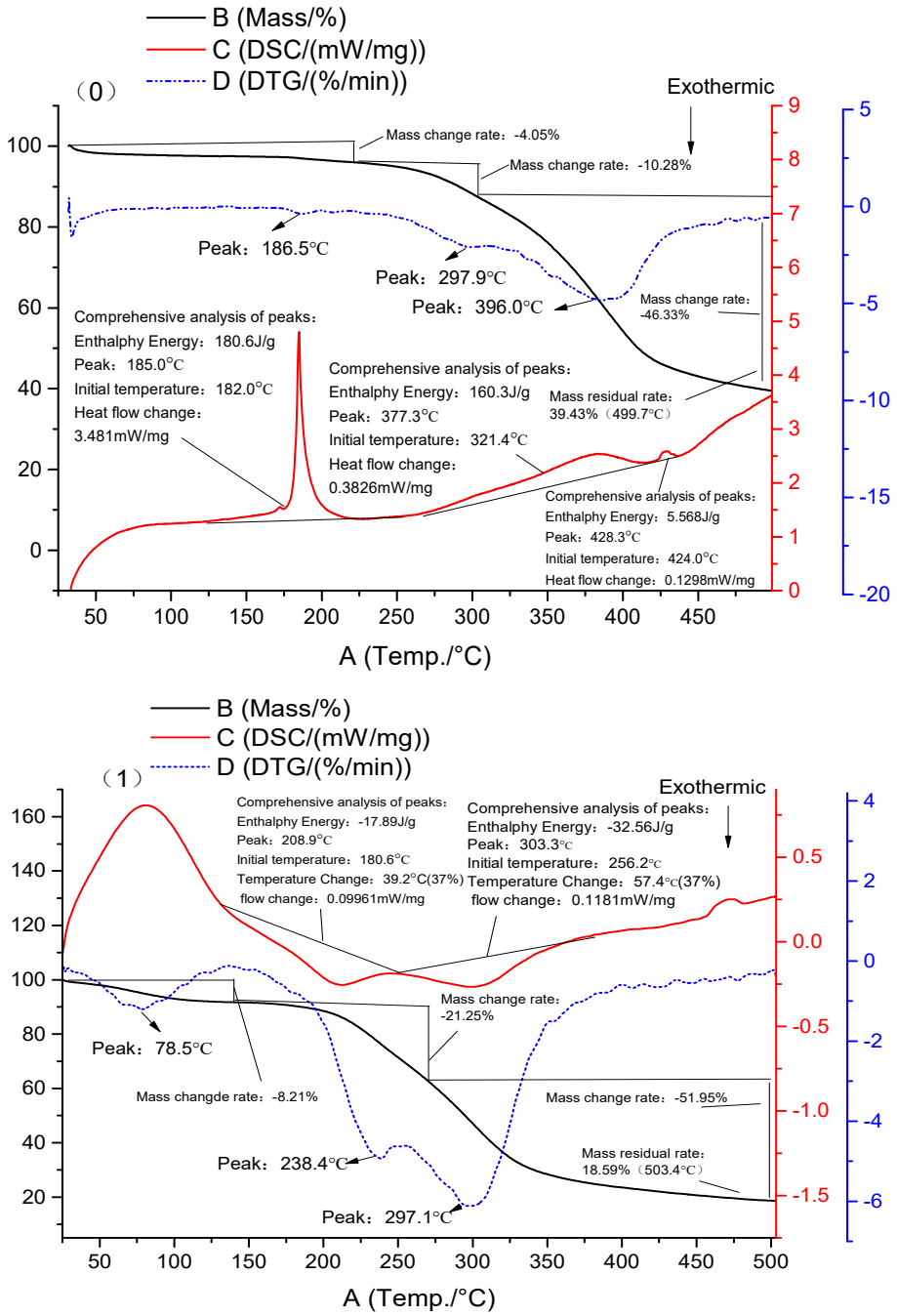

Figure 5. *Cont.*

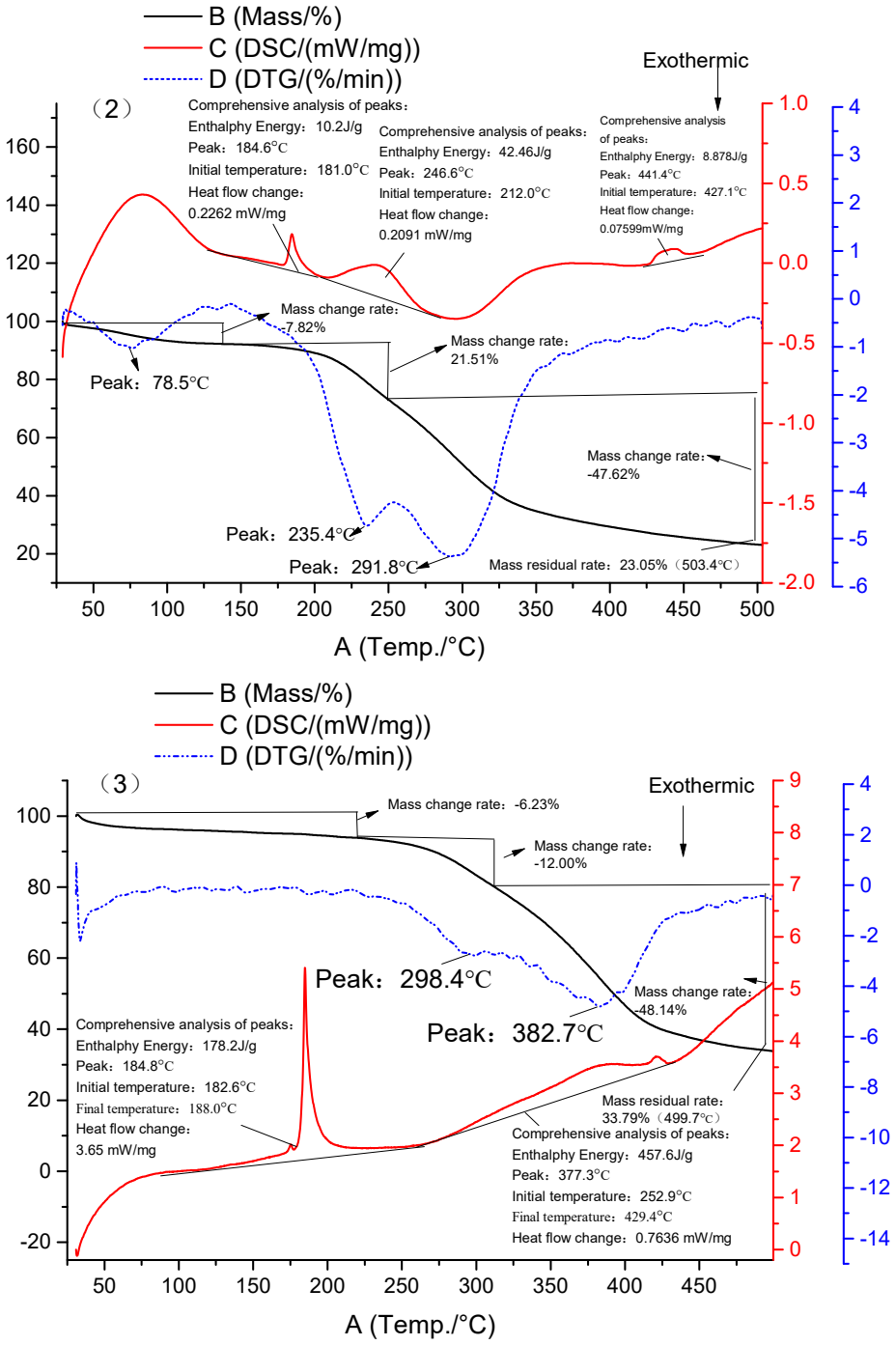

Figure 5. *Cont.*

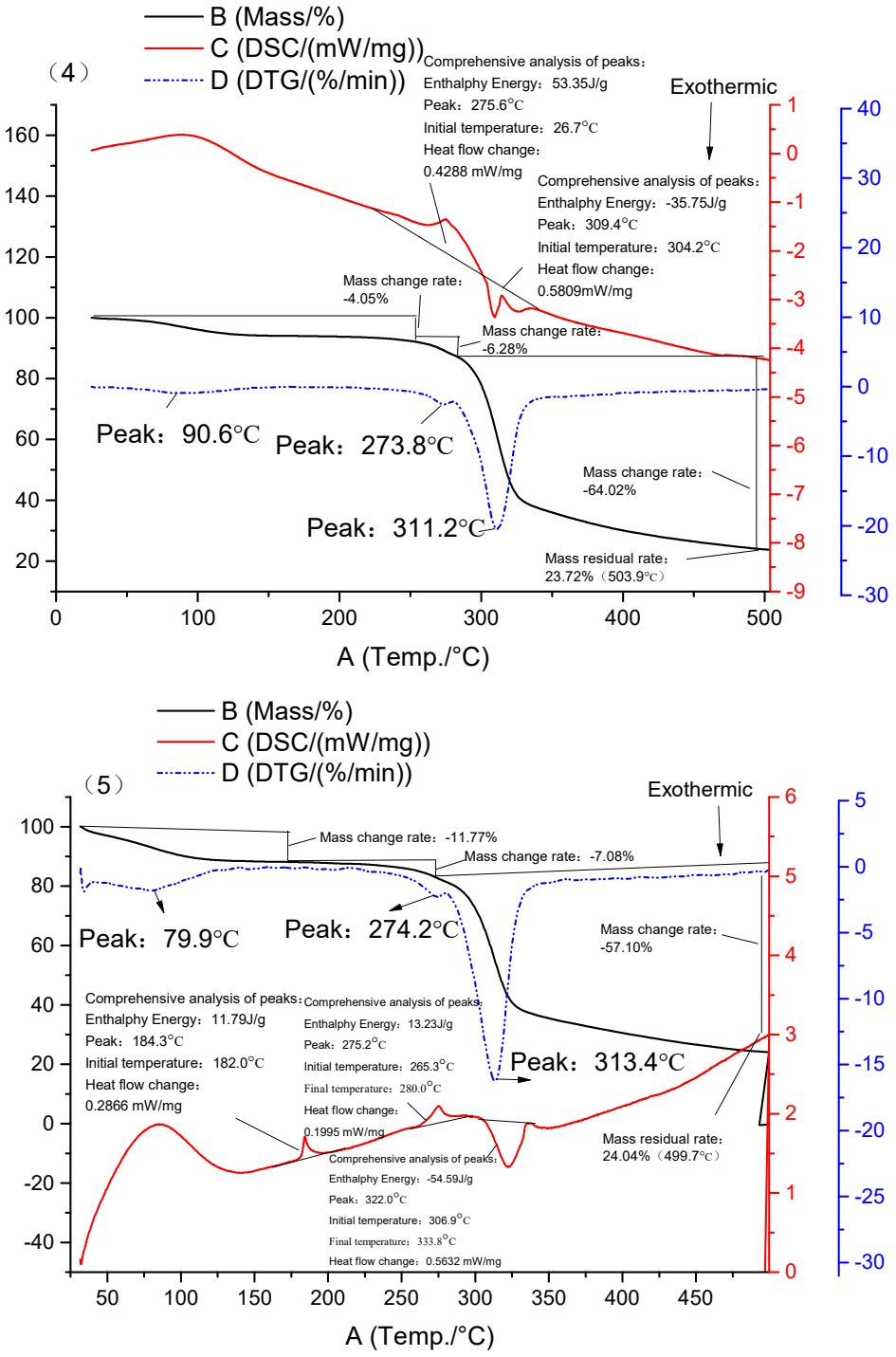

Figure 5. *Cont.*

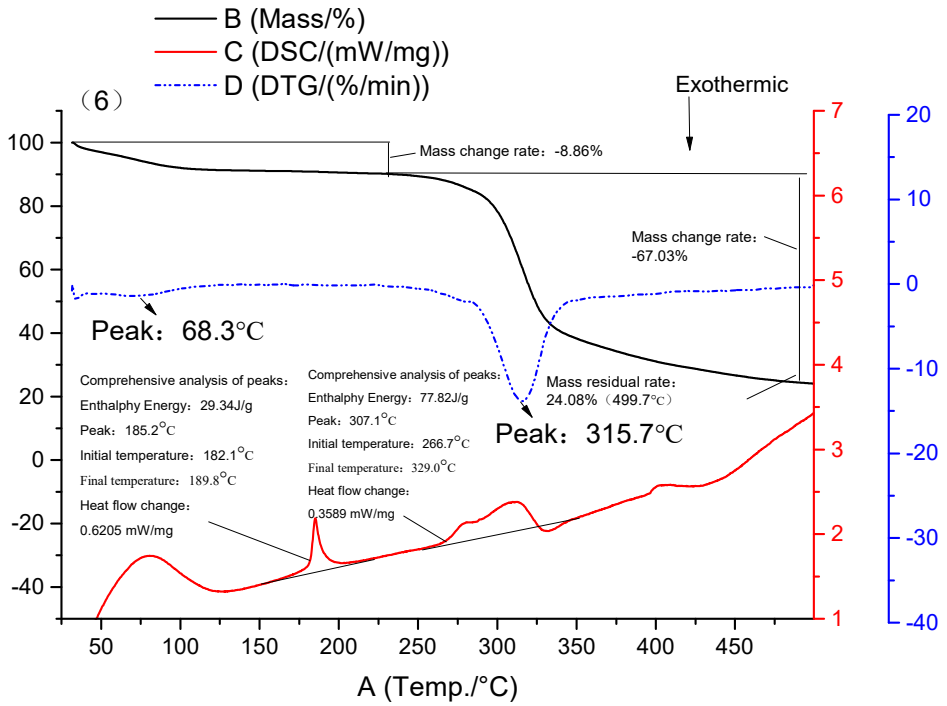

Figure 5. The thermal properties of (**0**) Curcumin, (**1**) LD, (**2**) LD-Cur mixtures, (**3**) LD-Cur complexes, (**4**) F-40, (**5**) F-40-Cur mixtures, and (**6**) F-40-Cur complexes.

The DSC spectrum [30] for the F-40-Cur complex showed two heat absorption peaks. The first heat absorption peak at 185.2 °C represented the heat absorption process of curcumin, which may also be caused by the amorphous part of F-40 or its interaction with the curcumin molecule. The second heat absorption peak near 307 °C represented the melting heat absorption process of the F-40-Cur complex. The heat absorption peak at 307 °C was higher than that of pure curcumin, F-40, the physical mixture of F-40-curcumin, and the LD-curcumin complex, indicating a stronger interaction between the two. More importantly, this observation demonstrates that LD could protect curcumin. A similar phenomenon was found in various cyclodextrin-curcumin complexes, and these complexes also provided better thermal protection of curcumin [31].

The thermogravimetry curves (TG) as well as the derivative thermogravimetry (DTG) of the pure curcumin sample, LD, LD-curcumin mixture, and LD-curcumin complex as well as F-40, F-40-Cur mixture, and F-40-Cur complex are shown in Figure 5. In the TGA curves of curcumin, no water loss was observed, probably due to its high hydrophobicity. For both the F-40 and LD samples, there were two stages of weight loss evident in the curves. The first one was observed near 100 °C, which was caused by the evaporation of water adsorbed on the LD, while the second stage of weight loss occurred in the range of 150 to 400 °C and was mainly characterized by the thermal degradation of LD and the evaporation of decomposition compounds. For LD, two narrow peaks were observed on the DTG curve, while for F-40, two broad peaks were observed in the range of 270 to 340 °C that were not separable. In addition, the degradation behavior of the F-40-Cur complex showed significant differences from that of the free curcumin and the LD-curcumin physical mixture, especially in the second phase, where degradation started at higher temperatures and occurred in a narrower temperature range. This phenomenon was consistent with the data from the DSC analysis, confirming the higher thermal stability of the LD-curcumin complex. The molecular interactions between LDs and ligands, the crystalline structure, and the aggregation behavior were strongly related to the molecular weight as well as the solubility.

3.5. Light Stability Analysis

The photodegradation curves of curcumin and LD-curcumin complexes as well as F-40-Cur complexes are shown in Figure 6. Curcumin contains a diketone structure, which is highly sensitive to light. Light can induce the degradation of active compounds. However, encapsulation techniques can improve the photostability of the active compound during storage. The photostability of the composites was evaluated under UV light conditions. After 60 h of UV irradiation, about 31% of curcumin in the pure sample was degraded, while only 13.9% of the curcumin complexes complexed with LD and 11.5% of the curcumin complexes complexed with F-40 were degraded after the same time period. The improved photochemical stability originated from the formation of intermolecular hydrogen bonds between curcumin and LD, which is consistent with the results reported by Mangolim et al. [2]. In addition, the retention of curcumin in the F-40-Cur complex was greater than that in the LD-curcumin complex. This result is consistent with the findings of Sun et al. [17]. Thus, the strength of the hydrophobic interaction between curcumin and LD significantly affects the photochemical stability of the complexes.

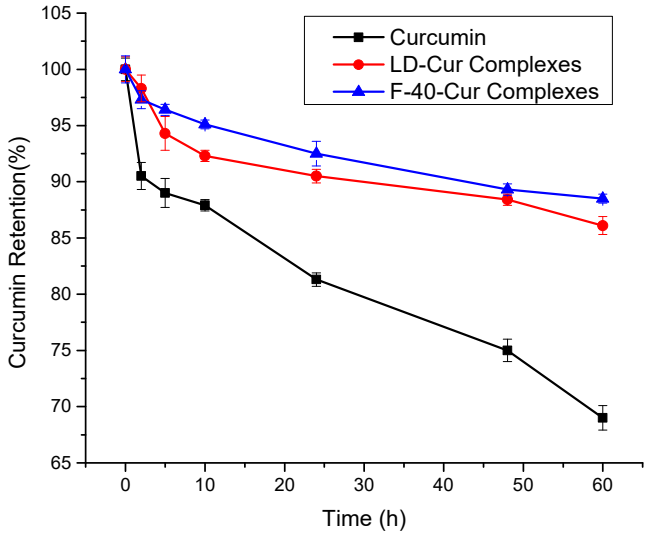

Figure 6. Detection of the optical stability of free curcumin, LD-Cur complexes, and F-40-Cur complexes.

3.6. In Vitro Simulation of Gastrointestinal Digestion Analysis

The in vitro release patterns of free curcumin, LD-curcumin complexes, and F-40-Cur complexes in simulated gastrointestinal fluid are shown in Figure 7. Curcumin possesses biological and pharmacological activities, especially in cancer proliferation and prevention [32]. Although curcumin has great efficacy in antitumors, its limited solubility and instability limit its application. The bioavailability of curcumin can be improved by its encapsulation [8]. While the release behavior of the LD-curcumin complex and the F-40-Cur complex in gastric juice was essentially stable, its release behavior in the intestinal fluid was noticeably different. As digestion proceeded, both complexes gradually released curcumin during stimulated gastric digestion, but the amount of curcumin in the stimulated gastric juice suggested different release profiles. The LD-curcumin complex released approximately 7.47% of curcumin after 1 h of stimulated gastric digestion, reached up to 11.37% after another 30 min of stimulated intestinal digestion, then decreased to 6.6% after a total of 180 min. Meanwhile, the F-40-Cur complex released about 7.90% of curcumin after 1 h of stimulated gastric digestion, reached up to 9.80% after another 30 min of stimulated intestinal digestion, and then decreased to 7.20% after a total of 180 min. Curcumin is known to be very unstable in aqueous environments, especially in media with pH values near or above 7. For this reason, it was inferred that the degradation of curcumin in simulated gastric juice leads to a decrease in cumulative release. The results of the in vitro release behavior are consistent with previously reported results [17]. Sun et al. confirmed the controlled

release performance of LD-curcumin composites, and the structural and physicochemical properties of the composites were related to the wall material, including chain length [17].

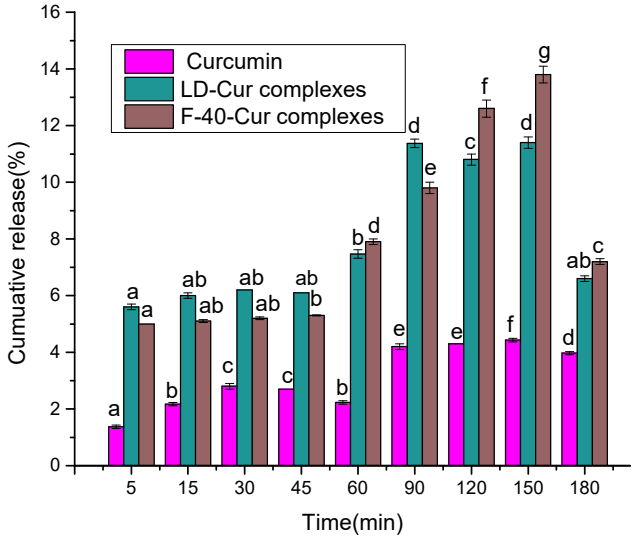

Figure 7. In vitro release patterns of pure curcumin, LD-Cur complexes, and F-40-Cur complexes. At different time points, different letters shown above the bars represent significant differences ($p < 0.05$). Conversely, bar graphs with the same letter marked at different time points represent no significant differences.

4. Conclusions

In conclusion, this work has demonstrated a facile strategy for preparing linear dextrin and curcumin complexes to improve the stability of curcumin. The molecular weight of LD directly affected the loading of curcumin, the encapsulation rate, and the yield of the complexes. Hydrogen bonding and hydrophobic interactions were the predominant interactions between LD and curcumin, whereas hydrogen bonding interactions were predominant between F-40 and curcumin. The molecular chain length facilitated the formation of their complexes. Curcumin was present in the complex in an amorphous form, and the thermal stability of curcumin to light was significantly enhanced in the complex after LD encapsulation. Compared to LD, long-chain F-40 was more effective at enhancing the photothermal protection of curcumin, allowing for a more efficient release of curcumin in the simulated intestinal fluid. More importantly, the thermal and photochemical stability of curcumin was dramatically enhanced with the formation of the complexes, and the curcumin was slowly released during gastrointestinal digestion in vitro.

Author Contributions: Conceptualization, H.X. and Q.G.; methodology, H.X.; software, H.X.; validation, H.X., Q.G. and L.M.; formal analysis, J.F.; investigation, Y.L.; resources, X.Y.; data curation, L.M.; writing—original draft preparation, H.X.; writing—review and editing, H.X.; visualization, Z.L.; supervision, Q.G.; project administration, Q.G.; funding acquisition, Q.G. All authors have read and agreed to the published version of the manuscript.

Funding: This study was financially supported by the Guangdong Basic and Applied Basic Research Foundation (2022A1515010354).

Conflicts of Interest: There is no conflict of interest.

References

1. Lestari, M.L.; Indrayanto, G. Curcumin. *Profiles Drug. Subst. Excip. Relat. Methodol.* **2014**, *39*, 113–204. [CrossRef] [PubMed]
2. Mangolim, C.S.; Moriwaki, C.; Nogueira, A.C.; Sato, F.; Baesso, M.L.; Neto, A.M.; Matioli, G. Curcumin-β-cyclodextrin inclusion complex: Stability, solubility, characterisation by FT-IR, FT-Raman, X-ray diffraction and photoacoustic spectroscopy, and food application. *Food Chem.* **2014**, *153*, 361–370. [CrossRef] [PubMed]
3. Mahady, G.B.; Pendland, S.L.; Yun, G.; Lu, Z.Z. Turmeric (Curcuma longa) and curcumin inhibit the growth of Helicobacter pylori, a group 1 carcinogen. *Anticancer Res.* **2002**, *22*, 4179–4181. [PubMed]

4. Reddy, R.C.; Vatsala, P.G.; Keshamouni, V.G.; Padmanaban, G.; Rangarajan, P.N. Curcumin for malaria therapy. *Biochem Biophys Res. Commun.* **2005**, *326*, 472–474. [CrossRef]
5. Wright, L.E.; Frye, J.B.; Gorti, B.; Timmermann, B.N.; Funk, J.L. Bioactivity of turmeric-derived curcuminoids and related metabolites in breast cancer. *Curr. Pharm. Des.* **2013**, *19*, 6218–6225. [CrossRef]
6. Vera-Ramirez, L.; Pérez-Lopez, P.; Varela-Lopez, A.; Ramirez-Tortosa, M.; Battino, M.; Quiles, J.L. Curcumin and liver disease. *Biofactors* **2013**, *39*, 88–100. [CrossRef]
7. Gupta, S.C.; Patchva, S.; Aggarwal, B.B. Therapeutic roles of curcumin: Lessons learned from clinical trials. *AAPS J.* **2013**, *15*, 195–218. [CrossRef]
8. Anand, P.; Kunnumakkara, A.B.; Newman, R.A.; Aggarwal, B.B. Bioavailability of curcumin: Problems and promises. *Mol. Pharm.* **2007**, *4*, 807–818. [CrossRef]
9. Aggarwal, B.B.; Harikumar, K.B. Potential therapeutic effects of curcumin, the anti-inflammatory agent, against neurodegenerative, cardiovascular, pulmonary, metabolic, autoimmune and neoplastic diseases. *Int. J. Biochem. Cell Biol.* **2009**, *41*, 40–59. [CrossRef]
10. Sun, A.; Shoji, M.; Lu, Y.J.; Liotta, D.C.; Snyder, J.P. Synthesis of EF24-tripeptide chloromethyl ketone: A novel curcumin-related anticancer drug delivery system. *J. Med. Chem.* **2006**, *49*, 3153–3158. [CrossRef]
11. Vemula, P.K.; Cruikshank, G.A.; Karp, J.M.; John, G. Self-assembled prodrugs: An enzymatically triggered drug-delivery platform. *Biomaterials* **2009**, *30*, 383–393. [CrossRef] [PubMed]
12. Namazi, H.; Dadkhah, A. Convenient method for preparation of hydrophobically modified starch nanocrystals with using fatty acids. *Carbohydr. Polym.* **2010**, *79*, 731–737. [CrossRef]
13. Angellier, H.; Molina-Boisseau, S.; Dole, P.; Dufresne, A. Thermoplastic starch-waxy maize starch nanocrystals nanocomposites. *Biomacromolecules* **2006**, *7*, 531–539. [CrossRef] [PubMed]
14. Xu, Y.; Ding, W.; Liu, J.; Li, Y.; Kennedy, J.F.; Gu, Q.; Shao, S. Preparation and characterization of organic-soluble acetylated starch nanocrystals. *Carbohydr. Polym.* **2010**, *80*, 1078–1084. [CrossRef]
15. Hewlings, S.J.; Kalman, D.S. Curcumin: A Review of Its Effects on Human Health. *Foods* **2017**, *6*, 92. [CrossRef]
16. Tiyaboonchai, W.; Tungpradit, W.; Plianbangchang, P. Formulation and characterization of curcuminoids loaded solid lipid nanoparticles. *Int. J. Pharm.* **2007**, *337*, 299–306. [CrossRef]
17. Sun, B. *Preparation, Phase Behavior and Application of Linear Dextrin*; Jiangnan University: Wuxi, China, 2018.
18. Xie, H.; Ma, X.; Lin, W.; Dong, S.; Liu, Q.; Chen, Y.; Gao, Q. Linear Dextrin as Potential Insulin Delivery System: Effect of Degree of Polymerization on the Physicochemical Properties of Linear Dextrin-Insulin Inclusion Complexes. *Polymers* **2021**, *13*, 4187. [CrossRef]
19. Marcolino, V.A.; Zanin, G.M.; Durrant, L.R.; Benassi Mde, T.; Matioli, G. Interaction of curcumin and bixin with β-cyclodextrin: Complexation methods, stability, and applications in food. *J. Agric. Food Chem.* **2011**, *59*, 3348–3357. [CrossRef]
20. Patel, A.; Hu, Y.; Tiwari, J.K.; Velikov, K.P. Synthesis and characterisation of zein-curcumin colloidal particles. *Soft Matter.* **2010**, *6*, 6192–6199. [CrossRef]
21. Pereira, A.G.B.; Fajardo, A.R.; Nocchi, S.; Nakamura, C.V.; Rubira, A.F.; Muniz, E.C. Starch-based microspheres for sustained-release of curcumin: Preparation and cytotoxic effect on tumor cells. *Carbohydr. Polym.* **2013**, *98*, 711–720. [CrossRef]
22. Kasapoglu-Calik, M.; Ozdemir, M. Synthesis and controlled release of curcumin-β-cyclodextrin inclusion complex from nanocomposite poly (N-isopropylacrylamide/sodium alginate) hydrogels. *J. Appl. Polym. Sci.* **2019**, *136*, 47554. [CrossRef]
23. Zeng, F.; Ma, F.; Gao, Q.; Yu, S.; Kong, F.; Zhu, S. Debranching and temperature-cycled crystallization of waxy rice starch and their digestibility. *Carbohydr. Polym.* **2014**, *113*, 91–96. [CrossRef] [PubMed]
24. Cohen, R.; Schwartz, B.; Peri, I.; Shimoni, E. Improving bioavailability and stability of genistein by complexation with high-amylose corn starch. *J. Agric. Food Chem.* **2011**, *59*, 7932–7938. [CrossRef] [PubMed]
25. Li, J.; Shin, G.H.; Lee, I.W.; Chen, X.; Park, H.J. Soluble starch formulated nanocomposite increases water solubility and stability of curcumin. *Food Hydrocoll.* **2016**, *56*, 41–49. [CrossRef]
26. Chai, Y.; Wang, M.; Zhang, G. Interaction between amylose and tea polyphenols modulates the postprandial glycemic response to high-amylose maize starch. *J. Agric. Food Chem.* **2013**, *61*, 8608–8615. [CrossRef]
27. Tang, B.; Ma, L.; Wang, H.-y.; Zhang, G.-y. Study on the Supramolecular Interaction of Curcumin and β-cyclodextrin by Spectrophotometry and Its Analytical Application. *J. Agric. Food Chem.* **2002**, *50*, 1355–1361. [CrossRef]
28. Pang, S.C.; Tay, S.H.; Chin, S.F. Facile synthesis of curcumin-loaded starch-maleate nanoparticles. *J. Nanomater.* **2014**, *2014*, 22. [CrossRef]
29. Klaochanpong, N.; Puttanlek, C.; Rungsardthong, V.; Puncha-arnon, S.; Uttapap, D. Physicochemical and structural properties of debranched waxy rice, waxy corn and waxy potato starches. *Food Hydrocoll.* **2015**, *45*, 218–226. [CrossRef]
30. Schick, C. Differential scanning calorimetry (DSC) of semicrystalline polymers. *Anal. Bioanal. Chem.* **2009**, *395*, 1589–1611. [CrossRef]
31. Sousdaleff, M.; Baesso, M.L.; Neto, A.M.; Nogueira, A.C.; Marcolino, V.A.; Matioli, G. Microencapsulation by freeze-drying of potassium norbixinate and curcumin with maltodextrin: Stability, solubility, and food application. *J. Agric. Food Chem.* **2013**, *61*, 955–965. [CrossRef]
32. Cabrespine-Faugeras, A.; Bayet-Robert, M.; Bay, J.-O.; Chollet, P.; Barthomeuf, C. Possible Benefits of Curcumin Regimen in Combination With Taxane Chemotherapy for Hormone-Refractory Prostate Cancer Treatment. *Nutr. Cancer* **2010**, *62*, 148–153. [CrossRef] [PubMed]